XLIV Jornadas de Automática 2023

CEA comité español de automática

XLIV Jornadas de AUTOMÁTICA 2023 — ZARAGOZA
https://jautomatica.es

A new approach for direct kinematic solution of a soft robotic neck

Nagua, L.[a,*], Monje, C.A.[a], Continelli, N.[a], Balaguer, C.[a]

[a] *Robotics Lab de la Universidad Carlos III de Madrid, Avda de la Universidad 30, 28911 Leganés, Madrid, Spain*

To cite this article: Nagua, L., Monje, C.A., Balaguer, C. 2023. A new approach for the direct kinematic solution of a soft robotic neck.
XLIV Jornadas de Automática, 697-701 https://doi.org/10.17979/spudc.9788497498609.697

Resumen

El mecanismo de cuello robótico presentado en este trabajo tiene como elemento principal un eslabón blando que emula un cuello humano con dos grados de libertad (DOF) (flexión, extensión y flexión lateral). El dispositivo se basa en un Mecanismo Paralelo Accionado por Cable (CDPM). Se desarrolla una cinemática directa a partir del sistema estático y la distribución geométrica del mecanismo, y se presentan ecuaciones lineales que permiten conocer fácilmente la longitud de los cables para hallar la posición del cuello, tanto en ángulos de inclinación como de orientación. Para el control del motor se utiliza un controlador PI de orden fraccionario (FOPI).

Palabras clave: Cuello robótico blando, Mecanismos paralelos accionados por cable (CDPM), Cinemática directa, Control de orden fraccionario.

A new approach for the direct kinematic solution of a soft robotic neck

Abstract

The robotic neck mechanism presented in this paper has as its main element a soft link that emulates a human neck with two DOF (flexion, extension and lateral bending). The mechanism is based on a Cable-Driven Parallel Mechanism (CDPM). A direct kinematics is developed from the static system and the geometric distribution of the mechanism, and linear equations are presented that relate the length of the cables and the position of the neck, both in inclination and orientation angles. For the motor control, a fractional order PI controller (FOPI) is used.

Keywords: Soft robotics neck, Cable-Driven Parallel Mechanisms (CDPM), Direct Kinematics, Fractional Order Control.

1. INTRODUCTION

Many animals have been an inspiration to simulate their physiological and group behavior. Soft robotics, which has developed rapidly in the last decades, has focused on the biology of animals, especially on their incredible locomotion and manipulation skills. For example, Wilson et al. (1993) review the motions of the squid tentacles and the elephant trunks and propose a design of a flexible arm manipulator with open loop control, Transeth et al. (2009) focuses on the locomotion of snake robots, and Mazzolai et al. (2012) create soft materials, mechanisms and actuators by simulating octopus arms. Important advancements have been made in the design of soft continuum robots Trivedi et al. (2008). Hirose studied the biomechanics of snakes leading to an interesting manipulator named “the elastic-module tendon-driven arm” Hirose and Yamada (2009).

Robotics has focused on simulating human movement through rigid mechanical mechanisms, but now, with soft robotics, it also replicates different human parts for the following main advantages: a) simplicity of design, favoring an under-actuated architecture; b) accessibility and adaptability to complex environments; and c) safer interaction with humans and the environment Nagua et al. (2018). In the mechanisms that simulate human necks on robots, two configurations stand out: series and parallel; the analysis of both configurations is presented in Nagua et al. (2018). Research has been conducted to

* Autor para correspondencia: lnagua@ing.uc3m.es

propose a new soft robotic neck design. Several designs of soft necks, whose workspaces have been analyzed, have been presented: Reinecke et al. (2016) describes a neck prototype with three DOF using a continuum mechanism based on tendons for actuation and the positions are generated by a kinematic mapping which assumes again a constant curvature. Another design proposal is presented in Gao et al. (2012), where a compression spring is used as a neck and it is actuated by four cables; with the lateral buckling motion of the spring, the kinematics can be solved.

Our review is motivated by the design presented in Nagua et al. (2018). As shown in Figure 1, the neck consists of a central mechanical soft link, which acts as the spine, and a parallel cable-driven mechanism, which allows the flexion of the central mechanical soft link.

In this paper we contribute to the solution of forward kinematics by solving the equations of the static system presented in Nagua et al. (2018); Continelli et al. (2023); and combined with the geometrical solution in the figure, the radius of curvature r from the center of the robot neck is related to the radius of curvature of each motor.

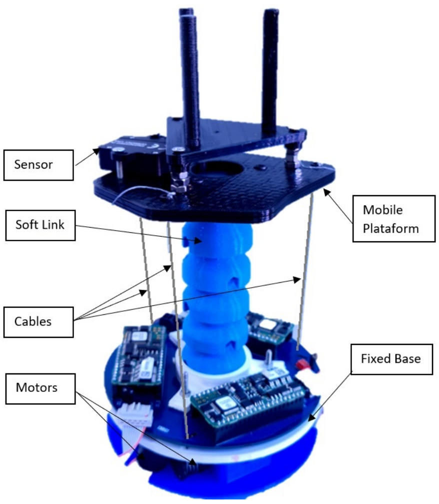

Figure 1: Soft neck platform

2. THE PLATFORM

All parts of the prototype can be built using 3D printing with PLA filament, except the soft link, that is built with NinjaFlex. In this case, the link has a weight of 20g for a payload of 600g, which means a ratio of 300% load to weight of the link (excluding all other parts of the prototype).

We have proposed a soft neck system driven by three cables, as shown in Figure 2. It has four main components: a fixed base, a mobile platform with coordinate frame $oxyz$, three cables with negligible mass and diameter, and a soft link.

The mobile platform is driven by the cables that are connected to the points B_i $(i = 1, 2, 3)$. The opposite end of each cable is connected to a motor DC that passes through the points A_i $(i = 1, 2, 3)$ of the fixed base with coordinate frame $OXYZ$. The X-axis and the x-axis are along OA_2 and oB_2, respectively, and the z-Z axes are perpendicular to the fixed base and the mobile platform respectively.

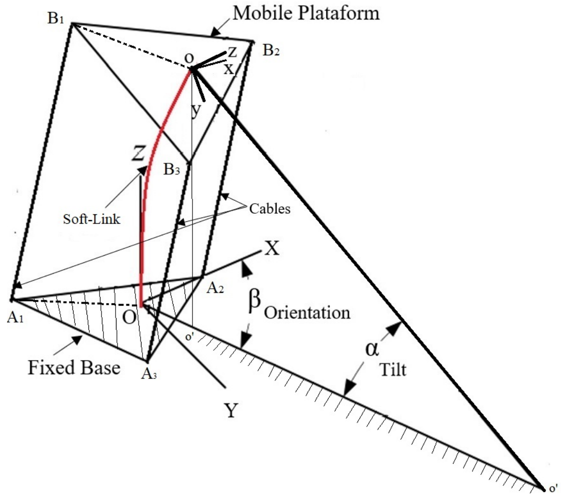

Figure 2: Schematic diagram of the soft robotic neck

3. STATIC SYSTEM

The soft neck has two independent parameters: angle α (tilt angle) and angle β (orientation angle). These parameters represent the position we want to obtain for the robotic neck as shown in Figure 2. We need to calculate the cable lengths L_i. Equation (1) represents the length of the cables necessary to obtain a given position Nagua et al. (2018),

$$L_i = \left\| {}^{O}T_{o'} \overrightarrow{oB_i} - \overrightarrow{OA_i} \right\| \quad (i = 1, 2, 3) \tag{1}$$

where:

- ${}^{O}T_{o'}$ is the homogeneous transformation matrix that represents the projection from $oxyz$ (mobile frame) to $OXYZ$ (fixed frame):

$$^{O}T_{o'} = \begin{bmatrix} ^{O}R_{o'} & P_o \\ 0 & 1 \end{bmatrix}$$

where:

- P_o is the position vector of point o with respect to the base coordinate frame and ${}^{O}R_{o'}$ is the rotational matrix that describes the orientation of the mobile platform using the Euler angles with ZYZ orientation.

$$^{O}R_{o'} = \begin{bmatrix} R_{11} & R_{12} & R_{13} \\ R_{21} & R_{22} & R_{23} \\ R_{31} & R_{32} & R_{33} \end{bmatrix}$$

- $\overrightarrow{oB_i}$ represents the points of the mobile platform.
- $\overrightarrow{OA_i}$ represents the points of the fixed base.

The cable forces acting on the mobile platform are represented by two perpendicular forces F_1 and F_2 in the plane Ost, and a moment M perpendicular to the plane at the upper center of the srping, as shown in Figure. 3. The mass of the mobile platform m is taken as a point at the upper center of the spring. The equilibrium of force and torque on the mobile platform Pham et al. (2005) is as follows:

$$\sum_{i=1}^{3} {}^{O}u_i\, T_i + F = 0 \tag{2}$$

$$\sum_{i=1}^{3} {}^{O}r_i \times {}^{O}u_i\, T_i + M = 0 \tag{3}$$

where:

$T_i = \begin{bmatrix} t_1, & t_2, & t_3 \end{bmatrix}^T$

${}^{O}u_i = ({}^{O}T_{o'}\overrightarrow{oB_i} - \overrightarrow{OA_i}) / \left\| {}^{O}T_{o'}\overrightarrow{oB_i} - \overrightarrow{OA_i} \right\|$

${}^{O}r_i = {}^{O}R_{o'} \cdot \overrightarrow{oB_i}$

$F = \begin{bmatrix} -F_1 \cos\beta, & -F_1 \sin\beta, & F_2 - mg \end{bmatrix}^T$

$M = \begin{bmatrix} -M \sin\beta, & M \cos\beta, & 0 \end{bmatrix}^T$

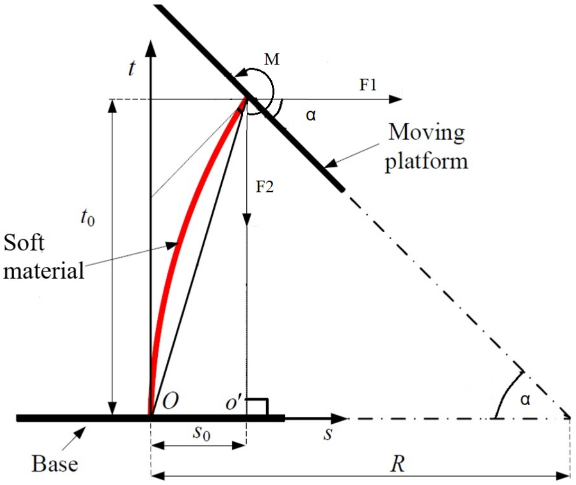

Figure 3: Force and torque of the system

Equation (2) can be decomposed into three equations:

$$t_1\ (R_{12}\, b + s_0\ \cos(\beta)) - t_2 \left(\frac{R_{12}\, b}{2} - \frac{\sqrt{3}\, a}{2} - s_0\ \cos(\beta) + \frac{\sqrt{3}\, R_{11}\, b}{2} \right) - t_3 \left(\frac{R_{12}\, b}{2} + \frac{\sqrt{3}\, a}{2} - s_0\ \cos(\beta) - \frac{\sqrt{3}\, R_{11}\, b}{2} \right) - F_1\ \cos(\beta) = 0 \tag{4}$$

$$t_2 \left(\frac{a}{2} - \frac{R_{22}\, b}{2} + s_0\ \sin(\beta) - \frac{\sqrt{3}\, R_{21}\, b}{2} \right) + t_3 \left(\frac{a}{2} - \frac{R_{22}\, b}{2} + s_0\ \sin(\beta) + \frac{\sqrt{3}\, R_{21}\, b}{2} \right) - F_1\ \sin(\beta) + t_1\ (R_{22}\, b - a + s_0\ \sin(\beta)) = 0 \tag{5}$$

$$F_2 + t_3 \left(t_0 - \frac{R_{32}\, b}{2} + \frac{\sqrt{3}\, R_{31}\, b}{2} \right) - g\, m - t_2 \left(\frac{R_{32}\, b}{2} - t_0 + \frac{\sqrt{3}\, R_{31}\, b}{2} \right) + t_1\ (t_0 + R_{32}\, b) = 0 \tag{6}$$

From (4) sin (β) - (5) cos (β), we have:

$$(a - b)\ (t_2\ \cos(\beta) - 2\, t_1\ \cos(\beta) + t_3\ \cos(\beta) - \sqrt{3}\, t_2\ \sin(\beta) + \sqrt{3}\, t_3\ \sin(\beta)) = 0 \tag{7}$$

From Equation (7), we have

$$\beta = \tan^{-1} \left(\frac{t_2 - 2\, t_1 - t_3}{\sqrt{3}\ (t_2 - t_3)} \right) \tag{8}$$

We know that:

$${}^{O}u_i = \frac{({}^{O}T_{o'}\overrightarrow{oB_i} - \overrightarrow{OA_i})}{\left\| {}^{O}T_{o'}\overrightarrow{oB_i} - \overrightarrow{OA_i} \right\|} = \frac{\overrightarrow{T_i}}{T_i}$$

Therefore, Equation (8) can be expressed as:

$$\beta = \tan^{-1} \left(\frac{L_2 - 2\, L_1 - L_3}{\sqrt{3}\ (L_2 - L_3)} \right) \tag{9}$$

4. GEOMETRY CONFIGURATION

In Section 3 the angle of orientation β was obtained with the static system of the mechanism, while now we will use the arc formed by the flexion of the soft link. Since it is not a perfect circular arc, for our study, we will consider an approximation. Our goal is to completely find a relationship between cable lengths and the position of soft robotic neck, which is useful for control systems.

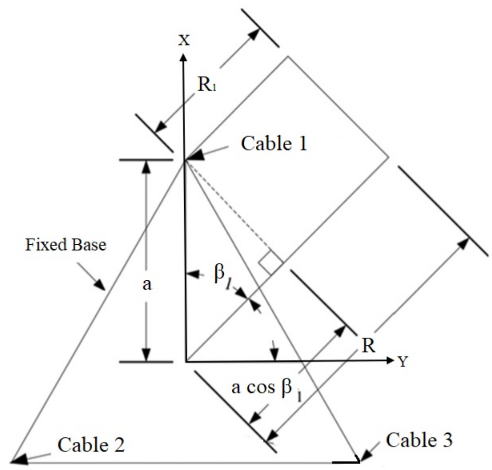

Figure 4: Diagram of the fixed base

Figure 2 provides a view of the fixed base and the mobile platform of the soft neck of the robot, while Figure 4 shows a view of the fixed base of the mechanism from above when looking down along the z-axis. As Figure 2 shows, the radius R of uniform curvature measured from the center of the neck is related to the radius R_i of curvature of each cable (L_2, L_1, L_3):

$$R_i = R - a\ \cos\beta_i \quad (i = 1, 2, 3) \tag{10}$$

where:

- a= distance from the center of the neck to one of the cables
- β_i = angle between soft link bending and cable i position

Considering the flexion of the soft link (see Figure 2) as an arc with a radius of curvature:

$$R = \frac{L_o}{\alpha} \tag{11}$$

where L_o is the length of the soft link.

By replacing (11) in (10) we get a relationship between the arc length of the robot L_o and the imaginary radius of the arc (L_{oi}):

$$R_i = \frac{L_o}{\alpha} - a \cos\beta_i \quad (i = 1, 2, 3) \tag{12}$$

Recalling that the length L_i of a chord formed with the extreme points of the arc L_{oi} is given by $L_i = 2R_i \sin\frac{\alpha}{2}$, therefore, the i^{th} equation of the cable length is:

$$L_i = 2 \sin\frac{\alpha}{2}\left(\frac{L_o}{\alpha} - a \cos\beta_i\right) \quad (i = 1, 2, 3) \tag{13}$$

The three cables are assumed to lie equally spaced around the soft link. Cables are separated by angles of 120^o (Figure 4) and are related to the plane Ost of the soft robotic neck by $\beta_1 = 90^o - \beta$, $\beta_2 = 210^o - \beta$ and $\beta_3 = 330^o - \beta$. Then, cables lengths are defined by the following equations:

$$L_1 = \sin\left(\frac{\alpha}{2}\right)\left(\frac{2\,L_0}{\alpha} - 2\,a\,\cos\left(\beta - \frac{\pi}{2}\right)\right) \tag{14}$$

$$L_2 = \sin\left(\frac{\alpha}{2}\right)\left(\frac{2\,L_0}{\alpha} - 2\,a\,\cos\left(\beta - \frac{7\,\pi}{6}\right)\right) \tag{15}$$

$$L_3 = \sin\left(\frac{\alpha}{2}\right)\left(\frac{2\,L_0}{\alpha} - 2\,a\,\cos\left(\beta - \frac{11\,\pi}{6}\right)\right) \tag{16}$$

Considering the expression ($L_2 - L_3$) of Equation (8), the subtraction of the equations (15) and (16) results as follows:

$$L_2 - L_3 = 2\sqrt{3}\,a\,\sin\left(\frac{\alpha}{2}\right)\cos(\beta) \tag{17}$$

Equation (17) can be expressed as:

$$\alpha = 2\sin^{-1}\left(\frac{L_2 - L_3}{2\sqrt{3}\,a\,\cos(\beta)}\right) \tag{18}$$

Now that all the relationships in (8) and (18) has been determined and the forward kinematics for the soft robotics neck have been described, we will validate it experimentally in the following section.

5. RESULTS

Figure 5 shows a pose control concept using the inclination (α) and orientation (β) angles of the soft robot neck. For a given pose of the neck (α,β $_{target}$), the angular displacements of each cable (θ_i) can be calculated from the inverse kinematics. These can be compared with the angular displacements measured by the encoders (θ_{si}) and the required deviation of the orientation angles (θ_e) can be calculated and given to the controller, for example, a Fractional Order Controller (FOC). The controller then calculates an appropriate angular velocity ω_r for the motor which, in turn, produces the system output.

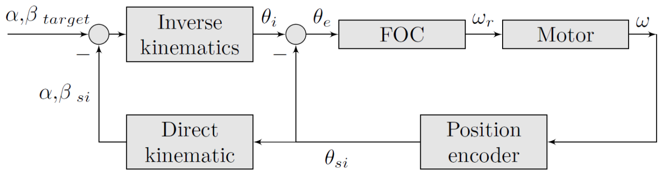

Figure 5: Closed loop control diagram for motors

The values from the encoders (θ_{si}) are also used to calculate the direct kinematics, giving the inclination and orientation (α,β $_{si}$) the soft robot neck, and these are compared with the target angles (α,β $_{target}$).

The test has a 15 degree inclination target (Figure 6) and an orientation of 0 to 90 degrees with steps of 22.5 degrees, as shown in Figure 7, and the different payloads attached to the mobile platform were $m = (0g, 500g)$.

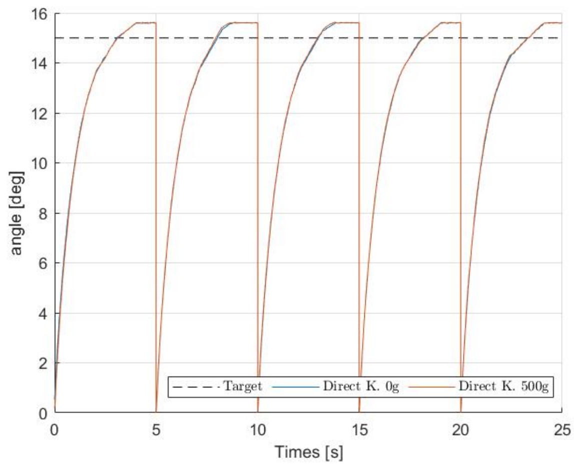

Figure 6: Neck inclination

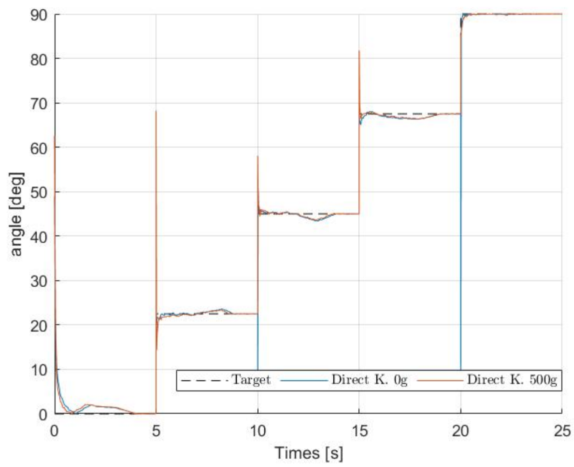

Figure 7: Neck orientation

As described in Mena et al. (2020), a fractional order PI controller is used to control each of the three motors on the platform, using the method described in Monje et al. (2008) for designing these controllers. This guarantees a robust control against uncertainties in the model and changes in the mass supported by the neck. The parameters obtained were kp = 0.2702503; ki = 1.4920678; ei = −0.9, resulting in the following controller transfer function:

$$C(s) = 0.2702503 + 1.4920678s^{-0.9} \tag{19}$$

From Figures 6 and 7, we can see that the solution given by the direct kinematic model proposed leads to the inclination and orientation targets, as measured by an IMU sensor placed at the top of the neck. Some small errors can be observed between the target and the reached position due to the fact that the model does not include the dynamics of the link, just the dynamics of the motors. This error can be corrected using an external control loop that feeds the IMU signal back to the system, as demonstrated in Mena et al. (2020).

Regarding direct kinematics solutions for parallel mechanisms, several proposals have been presented such as Nanua and Waldron (1989), Husty (1996), Pham et al. (2005). A disadvantage of these solutions is that their equations are nonlinear and therefore more computing resources are needed to compute them. In our research we present a new solution with linear equations.

The performance of the system can be viewed at: https://vimeo.com/366464057.

6. CONCLUSIONS

The direct kinematics problem of a soft robotic neck is analyzed in our research. In order to simplify the model, the approach looks for the relationship between the static system of forces and the geometric relationships of the mechanism. This results in three linear equations relating the cable lengths with the inclination and orientation of the soft neck. The kinematics has been validated experimentally using a fractional order PI controller to command the motors of the system.

Acknowledgements

The research leading to these results has received funding from the project SOFIA: Articulación blanda inteligente con capacidades de reconfiguración y modularidad para plataformas robóticas, with reference PID2020-113194GB-I00, funded by the Spanish Ministry of Economics, Industry and Competitiveness

References

Continelli, N. A., Nagua, L. F., Monje, C. A., Balaguer, C., 2023. Modelado de un cuello robótico blando mediante aprendizaje automático. Revista Iberoamericana de Automática e Informática industrial.

Gao, B., Xu, J., Zhao, J., Xi, N., 2012. Combined inverse kinematic and static analysis and optimal design of a cable-driven mechanism with a spring spine. Advanced Robotics 26 (8-9), 923–946.

Hirose, S., Yamada, H., 2009. Snake-like robots [tutorial]. IEEE Robotics & Automation Magazine 16 (1), 88–98.

Husty, M. L., 1996. An algorithm for solving the direct kinematics of general stewart-gough platforms. Mechanism and Machine Theory 31 (4), 365–379.

Mazzolai, B., Margheri, L., Cianchetti, M., Dario, P., Laschi, C., 2012. Soft-robotic arm inspired by the octopus: Ii. from artificial requirements to innovative technological solutions. Bioinspiration & biomimetics 7 (2), 025005.

Mena, L., Monje, C. A., Nagua, L., Muñoz, J., Balaguer, C., 2020. Test bench for evaluation of a soft robotic link. Frontiers in Robotics and AI 7, 27.

Monje, C. A., Vinagre, B. M., Feliu, V., Chen, Y., 2008. Tuning and auto-tuning of fractional order controllers for industry applications. Control engineering practice 16 (7), 798–812.

Nagua, L., Muñoz, J., Monje, C. A., Balaguer, C., Sep 2018. A first approach to a proposal of a soft robotic link acting as a neck. In: Actas de las Jornadas de Automática. Área de Ingeniería de Sistemas y Automática, Universidad de Extremadura, pp. 522–529.

Nanua, P., Waldron, K. J., 1989. Direct kinematic solution of a stewart platform. In: Proceedings, 1989 International Conference on Robotics and Automation. IEEE, pp. 431–437.

Pham, C. B., Yeo, S. H., Yang, G., 2005. Tension analysis of cable-driven parallel mechanisms. In: 2005 IEEE/RSJ International Conference on Intelligent Robots and Systems. IEEE, pp. 257–262.

Reinecke, J., Deutschmann, B., Fehrenbach, D., 2016. A structurally flexible humanoid spine based on a tendon-driven elastic continuum. In: 2016 IEEE International Conference on Robotics and Automation (ICRA). IEEE, pp. 4714–4721.

Transeth, A. A., Pettersen, K. Y., Liljebäck, P., 2009. A survey on snake robot modeling and locomotion. Robotica 27 (7), 999–1015.

Trivedi, D., Rahn, C. D., Kier, W. M., Walker, I. D., 2008. Soft robotics: Biological inspiration, state of the art, and future research. Applied bionics and biomechanics 5 (3), 99–117.

Wilson, J., Li, D., Chen, Z., George, R., 1993. Flexible robot manipulators and grippers: Relatives of elephant trunks and squid tentacles. In: Robots and Biological Systems: Towards a New Bionics? Springer, pp. 475–494.